Journal of Applied Polymer Science

Operating Window of Solution Casting. II. Non-Newtonian Fluids

Yuan-Chang Huang,[1] Tai-Zan Wang,[1] Ta-Jo Liu,[1] Carlos Tiu[2]
[1]Department of Chemical Engineering, National Tsing Hua University, Hsinchu 30043, Taiwan, Republic of China
[2]Department of Chemical Engineering, Monash University, Victoria 3800, Clayton, Australia
Correspondence to: T.-J. Liu (E-mail: tjliu@che.nthu.edu.tw)

ABSTRACT: The operating windows of the solution casting of two polymeric liquids were evaluated experimentally. The experimental setup and procedure were the same as used previously for the casting of Newtonian fluids (*Journal of Applied Polymer Science* 2013, 129, 507–516). Aqueous carboxymethylcellulose/glycerol solutions exhibited pure shear-thinning behavior at low polymer concentrations but became viscoelastic at high polymer concentrations, whereas polyacrylamide/glycerol solutions showed viscoelastic behavior over a wide range of concentrations. The shear-thinning behavior, in conjunction with a low level of elasticity, of the casting solution was found to be useful in expanding the stable operating windows. However, an opposite effect on the operating windows was found for highly elastic solutions. The non-Newtonian effect on the maximum stable casting speed was prominent only when the capillary number exceeded unity. Defects outside of the operating window were mostly similar to those observed in Newtonian solution casting. For highly concentrated solutions, a new rough surface defect was observed. This defect could be attributed to polymer chain entanglement, alignment, or breakup. © 2014 Wiley Periodicals, Inc. J. Appl. Polym. Sci. **2015**, *132*, 41411.

KEYWORDS: coatings; rheology; viscosity and viscoelasticity

Received 10 June 2014; accepted 14 August 2014
DOI: 10.1002/app.41411

INTRODUCTION

Many industrial polymer films are made by the solvent or solution casting process.[1] Some of these films include polyimide (PI) films[2–11] and triacetyl cellulose (TAC) films,[12–18] which are widely used in optical electronic applications. The solution casting process is suitable for the fabrication of temperature-sensitive polymer films. High-uniformity films can be produced with excellent optical properties and low haze. Early patents and studies on solution casting have mainly focused on the production of celluloid films.[19–21] Recently, major research efforts have been focused on the production of PI and TAC films through solution casting. Hamamoto et al.[4] suggested that PI films could be made with high tensile strength and elongation through solution casting operations. Hungerford[10] attempted to make an optically clear, highly oriented PI film with high electrical resistance, flexibility, and strength. Okahashi et al.[5] proposed to the production of isotropic PI films with solution casting. Asakura et al.[3] developed aromatic PI films with high thermal and mechanical properties for flexible printed circuits. Kohn[11] suggested that ultrathin and pinhole-free PI films could be made with the solution casting processes. Several authors have also studied the optical birefringence of TAC films.[16,22,23]

Three major steps involved in solution casting are liquid film casting, solvent removal, and the peeling of dried films from the steel belt. Despite the importance of solution casting in polymer processing operations, the fundamental analysis of this process appears to be limited. Solution casting bears some resemblance to slot die coating[24–27] and curtain coating[24,25,28,29] operations. Usually, the solutions used in casting have higher viscosities than those used in slot die and curtain coatings, and the gap between the cast die and the moving substrate is larger than that in slot die coating but smaller than that in curtain coating. Hence, the fluid mechanics and flow phenomena of casting and coating are expected to be significantly different.

Huang et al.[30] studied the fluid mechanics of Newtonian fluids in solution casting. They determined the stable operating windows in terms of the maximum operating speed as functions of the material properties and operating variables. This study is an extension of previous work on non-Newtonian fluids. The test fluids were aqueous glycerol solutions of carboxymethylcellulose (CMC) and polyacrylamide (PAA). The effects of shear thinning and the viscoelasticity on the stable operating windows and the casting defects were examined.

EXPERIMENTAL

The slot die used in this study was the same as that used in a previous work.[30] The casting solution emanated from the slot die and was deposited on a moving poly(ethylene terephthalate)

Table I. Physical Properties of the Test Solutions [CMC (DS = 0.7) and PAA Aqueous Solutions] with Different Glycerol Concentrations

Code	Concentration of glycerol (wt %)	MW of CMC	Concentration of the Test Solution (ppm)	Density (kg/m^3)	Surface tension (mN/m)
CMC aqueous solutions					
A	90	—	0	1.233×10^3	62.4
CMC-1	90	250×10^3	100	1.232×10^3	64
CMC-2	90	250×10^3	500	1.233×10^3	64.2
CMC-3	90	250×10^3	1000	1.230×10^3	64
CMC-4	90	250×10^3	1500	1.252×10^3	64.1
CMC-5	90	250×10^3	2000	1.240×10^3	63.8
CMC-6	90	250×10^3	3000	1.250×10^3	63.9
CMC-7	96.7	90×10^3	1000	1.252×10^3	~64
CMC-8	84.5	700×10^3	1000	1.220×10^3	~64
PAA aqueous solution					
PAA-1	91	—	60	1.245×10^3	64.4
PAA-2	90	—	100	1.242×10^3	64.3
PAA-3	89	—	120	1.240×10^3	63.7
PAA-4	98	—	60	1.240×10^3	63.5
PAA-5	98	—	100	1.260×10^3	63.6
PAA-6	97	—	120	1.256×10^3	63.8
PAA-7	50	—	1500	1.150×10^3	60.5

substrate. The quality of the liquid film on the substrate was measured. Several blades were used to remove the cast liquid film from the substrate. The substrate was then washed, dried, and rewound. The proper design of the slot die was critical for the successful casting operation.

The test fluids were aqueous glycerol solutions of CMC and PAA. Three different molecular weights (MWs) and various degrees of substitution (DSs) of CMC were used. These MWs were 90,000, 250,000, and 700,000. The polymers were supplied by Acros Organics (catalog numbers 332600010, 332610010, 332620010, 332630010, and 332640010). In addition, two different PAA polymers with MWs of 5,000,000–6,000,000 and 18,000,000 were supplied (Polyscience, catalog numbers 02806-250 and 18522-100). The molecular structures of the two polymers were different, with CMC being semirigid and PAA being flexible. Glycerol (Uni-Onward Co., XR-LGLY-20L) was added to both polymer solutions to serve as a viscosity thickener. The PAA solution with a high glycerol content exhibited a constant viscosity and was elastic, which is characteristic of the ideal elastic fluid developed by Boger.[31] The procedure used by Tam et al.[32] was followed for the preparation of the PAA/glycerol solutions.

The poly(ethylene terephthalate) substrate was produced by Nan Ya Plastic Co. (code BH-21). The film had a thickness of 50 μm and a surface energy of 38.9 mJ/m^2. The contact angle with water was 69.2°. All of the physical properties of the test solutions were measured before the flow experiments. The surface tension was determined by a surface tensiometer (Kyowa Interface Science, CBVP-A3). The steady shear viscosity (η) and the first normal stress difference (N_1) as functions of the shear rate ($\dot{\gamma}$) were measured with a cone-and-plate rheometer (TA Instruments, ARES-LS1). All of the physical data of the test solutions are given in Table I.

RESULTS AND DISCUSSION

The CMC solutions were tested first to examine the effects of their physical and rheological properties on the operating window. The rheological properties of the CMC solutions were functions of the polymer and glycerol concentrations, DS, and MW of the polymer.

It was reported that DS has little effect on the rheological properties of CMC solutions,[33] and this was confirmed in this study. The effects of other physical and molecular properties are presented here. Figure 1 shows the effects of the CMC concentration on η

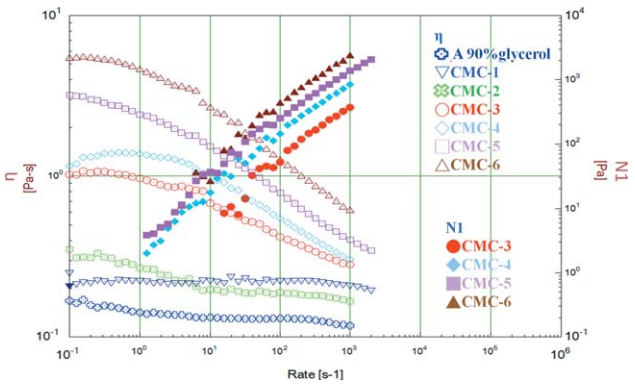

Figure 1. Rheological properties, η and N_1, of the CMC solutions with different concentrations (DS = 0.7, MW = 250 × 10^3, and 90% glycerol). [Color figure can be viewed in the online issue, which is available at wileyonlinelibrary.com.]

Table II. Rheological Properties of the CMC and PAA Aqueous Solutions

	$\eta=\mu_0^{\dot{\gamma}^{n-1}}$		$N_1=a^{\dot{\gamma}^m}$	
Code	μ_0 (mPa s)	n	a (Pa)	m
A	250	~1	—	—
CMC-1	139.95	0.968	—	—
CMC-2	274.0	0.919	—	—
CMC-3	1.11×10^3	0.801	1.36	0.825
CMC-4	1.56×10^3	0.773	4.25	0.780
CMC-5	1.64×10^3	0.765	[a]	[a]
CMC-6	5.45×10^3	0.670	[a]	[a]
CMC-7	1.15×10^3	0.91	0.69	0.90
CMC-8	1.03×10^3	0.756	3.38	0.744
PAA-1	346.24	0.93	0.04	1.08
PAA-2	348.23	0.92	0.11	0.99
PAA-3	371.21	0.91	1.27	0.87
PAA-4	1.02×10^3	0.98	0.50	0.90
PAA-5	1.48×10^3	0.92	1.20	0.86
PAA-6	1.21×10^3	0.94	10.47	0.99

An em dash indicates that we could not detect the value because N_1 was too low.
[a] No operating windows.

and N_1. The effect of shear thinning was more prnounced with increasing CMC concentration. The CMC solution was not known to be elastic at low polymer MW and concentration. N_1 was detectable only for the high-MW polymer solutions and at concentrations greater than 500 ppm. Values of N_1 also increased with the CMC concentration over the same $\dot{\gamma}$ ranges. As shown in Table I, the density and surface tension remained relatively constant regardless of the polymer concentration. A simple rheological power law model could be used to fit the η and N_1 data as follows:

$$\tau=\mu_0\dot{\gamma}^n \quad or \quad \eta=\mu_0\dot{\gamma}^{n-1} \tag{1a}$$

$$N_1=a\dot{\gamma}^m \tag{1b}$$

where τ is the shear stress and constant a characterize elasticity property. The values of the fitted parameters, zero shear rate viscosity μ_0, power law index for viscosity n, and power law index for elasticity m, for the CMC solutions are given in Table II. We noted that the values of n and m were very close; this indicated that the variations in η and the elasticity with $\dot{\gamma}$ were similar.

The effect of MW was examined with three 1000-ppm CMC solutions with different MWs (CMC-3, CMC-7, and CMC-8, respectively). The rheological properties of the three solutions are presented in Figure 2 and Table II. The fluid consistency (μ_0) was maintained at around 1100 mPa s through adjustment of the quantity of glycerol added. As shown in Figure 2, the zero-η values of the three solutions appeared to approach each other but deviated significantly in their shear-thinning and elastic regions; this depended on the polymer MW. Of the three solutions, the one having the highest polymer MW (CMC-8) exhibited the highest degree of shear thinning and the largest value of N_1 over the same $\dot{\gamma}$ region.

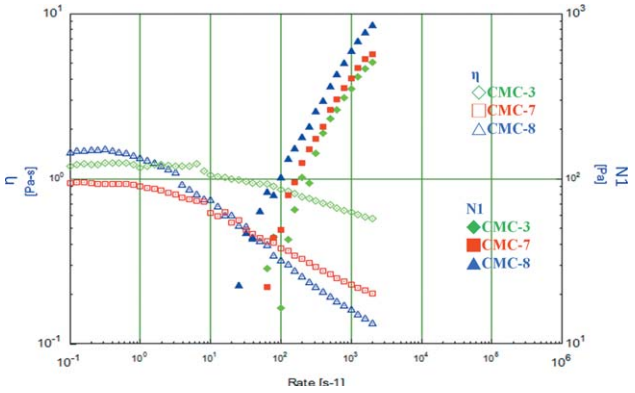

Figure 2. Rheological properties, η and N_1, of the CMC solutions with three different MWs at zero shear rate viscosity $\eta_0 \approx 1100$ mPa s (DS = 0.7 and concentration = 1000 ppm). [Color figure can be viewed in the online issue, which is available at wileyonlinelibrary.com.]

The effect of the CMC concentration on the operating windows is shown in Figure 3 for the three different casting gaps (*Hs*). For mildly elastic fluids, the operating windows were larger

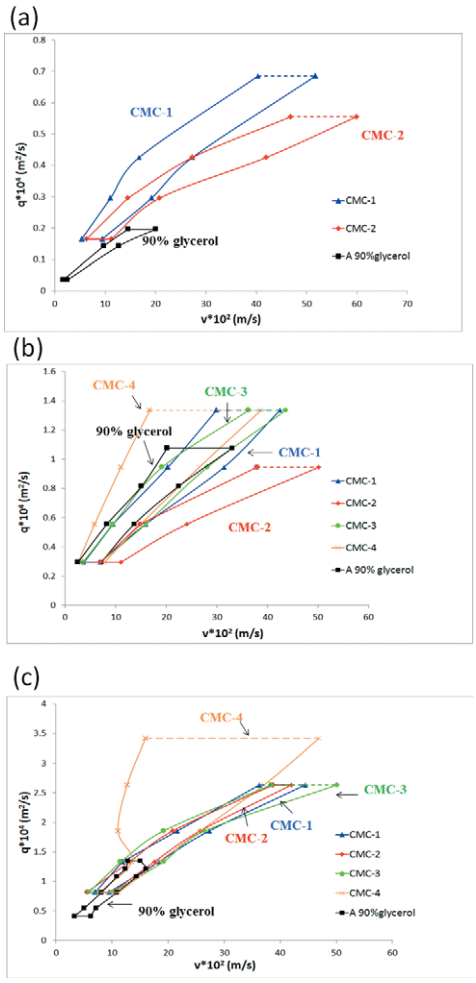

Figure 3. Operating windows of the CMC solutions with different concentrations and *Hs* (MW = 250 × 10^3, DS = 0.7, and 90% glycerol): H = (a) 200, (b) 500, and (c) 1000 μm. (q is flow rate/unit casting width and v is casting speed) [Color figure can be viewed in the online issue, which is available at wileyonlinelibrary.com.]

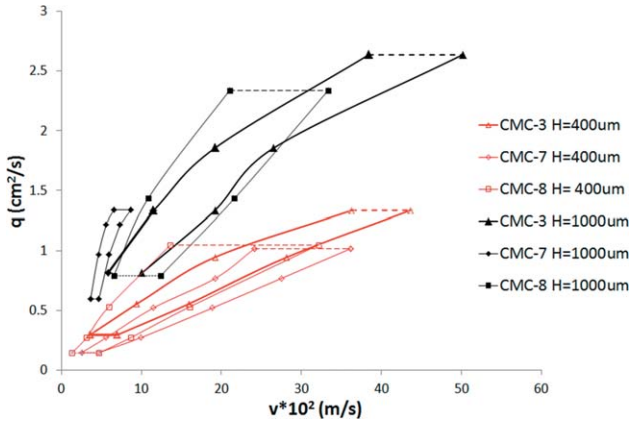

Figure 4. Operating windows of the 1000-ppm CMC solutions with different MWs at $H = 400$ and 1000 μm. (q is flow rate/unit casting width and v is casting speed) [Color figure can be viewed in the online issue, which is available at wileyonlinelibrary.com.]

than those obtained for purely viscous fluids. In contrast, an opposite phenomenon was observed for highly elastic fluids.[34,35] Figure 3(a) shows that the casting of a mildly elastic, shear-thinning solution (either CMC-1 or CMC-2) resulted in a significant expansion of the operating window. For a small H (200 μm), the effect of N_1 was more pronounced because of the higher apparent shear rate ($\dot{\gamma}_{max}$). A stable operating window could not be obtained when the CMC concentration exceeded 1000 ppm because of the high fluid elasticity. However, it was possible to obtain an operating window for the same CMC solution when H was increased to 500 μm. For the larger H, $\dot{\gamma}_{max}$ was only half of that for the smaller H at the same casting speed. Hence, the impact of the elasticity was only marginal. An optimum operating window appeared to exist with a certain concentration of CMC solution having a proper combination of viscous and elastic characteristics. Once the optimum concentration was exceeded, the elastic effect became predominant, and this resulted in a contraction of the operating window and the appearance of casting defects. Figure 3(b) displays the casting windows of various CMC solutions obtained with an H of 500 µm. The operating window reached its largest size at a CMC concentration of around 500 ppm. The optimal concentration shifted to around 1000 ppm when H was increased to 1000 μm, as indicated in Figure 3(c).

Figure 4 shows the effect of the MW of CMC on the operating windows obtained for three CMC solutions (CMC-3, CMC-7, and CMC-8) at two different Hs. For the smaller H (400 μm), the operating window obtained for CMC-7 was the largest, as the solution was only slightly elastic at a high shear flow. For the larger H (1000μm), the same solution yielded the smallest operating window because $\dot{\gamma}$ was significantly lower when the effect of the fluid elasticity was negligible. Under the same flow conditions, the CMC solution with the intermediate MW (CMC-3) was mildly elastic; this effect was responsible for the window expansion. On the other hand, the elasticity level for the solution of high MW (CMC-8) was still strong enough to cause the window to contract.

The maximum capillary number (Ca_{max}), defined in terms of the maximum stable operating velocity (V_{max}) and surface tension (σ), is given by

$$Ca_{max} = \frac{\eta V_{max}}{\sigma} = \frac{\mu_0(\dot{\gamma}_{max})^{n-1}\dot{\gamma}_{max}}{\frac{\sigma}{H}} \quad (2)$$

where $\dot{\gamma}_{max}$ is

$$\dot{\gamma}_{max} = \frac{v_{max}}{H} \quad (3)$$

Figure 5 shows the plots of Ca_{max} against H for various CMC solutions. The operating window appeared to be influenced only by the fluid elasticity when Ca_{max} exceeded unity. Because of the difference in the elasticity level, the largest operating windows at $H = 500$ and $H = 1000$ µm were obtained for the CMC-7 and CMC-4 solutions, respectively. When Ca_{max} was less than unity, there was very little effect of the fluid elasticity on the operating window.

An attempt was made to quantify the relative importance of the elastic and viscous forces in solution casting with the local Weissenberg number (Wi), and we evaluated at the local maximum casting speed for a flow rate (V_a). Wi was defined as the ratio of N_1 to τ, as follows:

$$Wi = \frac{N_1}{\tau} = \frac{N_1}{\mu_0(\dot{\gamma}_a)^{n-1}\dot{\gamma}_a} \quad (4)$$

The local maximum speed of Ca was calculated as follows:

$$Ca = \frac{\eta v_a}{\sigma} = \frac{\mu_0(\dot{\gamma}_a)^{n-1}\dot{\gamma}_a}{\frac{\sigma}{H}} \quad (5)$$

where apparent shear rate ($\dot{\gamma}_a$) = V_a/H.

Many researchers have adopted either a critical Deborah number or a Wi to characterize the onset of the flow instability in free surface flow.[36] Figure 6 shows plots of Wi against Ca for four CMC solutions at various Hs. For each CMC solution, Wi appeared to increase with increasing polymer MW and concentration but independent of Ca. The values of Wi were above unity for the CMC-3, CMC-4, and CMC-8 solutions. The values of Wi of the CMC-8 (1000-ppm) solution were smaller than those of the CMC-4 (1500-ppm) solution, although the

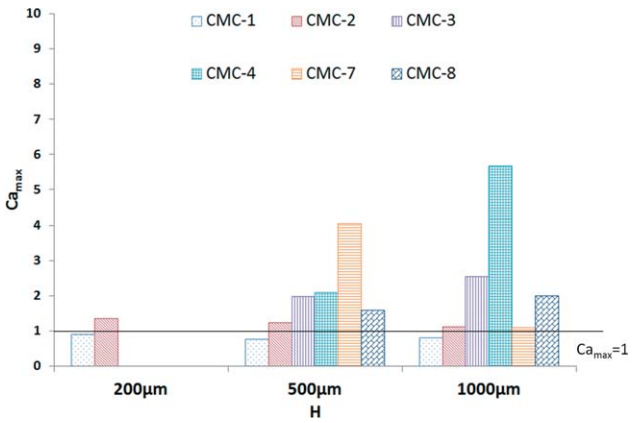

Figure 5. Ca_{max} values of the different CMC solutions. [Color figure can be viewed in the online issue, which is available at wileyonlinelibrary.com.]

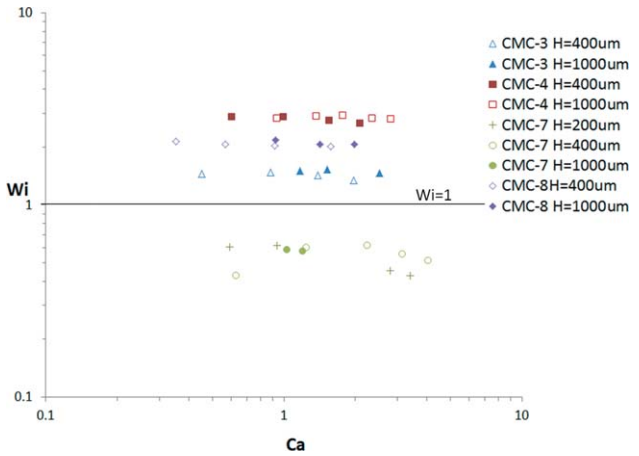

Figure 6. Wi versus Ca for the different CMC solutions. [Color figure can be viewed in the online issue, which is available at wileyonlinelibrary.com.]

MW of CMC-8 was higher. This suggested concentration effect was stronger than the MW effect on Wi.

To further assess the impact of the elasticity on the operating window, the casting experiment was repeated with six high-molecular-weight PAA glycerol solutions with different PAA concentrations. The composition and physical properties of these six solutions (PAA-1 to PAA-6) are listed in Table I. The rheological behaviors of these solutions are shown in Figure 7, with the power law parameters given in Table II. All of these solutions exhibited mild shear thinning but significant elastic characteristics. The rheological characteristics of these solutions resembled those of a Boger fluid.[31]

The effect of H on the operating windows of the PAA solutions was examined. For an H of 200 μm, we found that the fluid elasticity increased substantially at high $\dot{\gamma}$ s in the flow regime between the die and the moving substrate. A ribbing defect was observed for highly concentrated PAA solutions. It was not possible to obtain any stable operating window when the concentration of PAA exceeded 100 ppm. Stable operating windows could only be obtained for solutions with PAA concentration below 60 ppm. The defects observed outside the operating window for these solutions were stable pooling and air entrainment in the low- and high-speed limits, respectively. When H was increased to 400 μm or larger, the average $\dot{\gamma}_{max}$ in the similar flow regime decreased, and this resulted in a larger operating window.

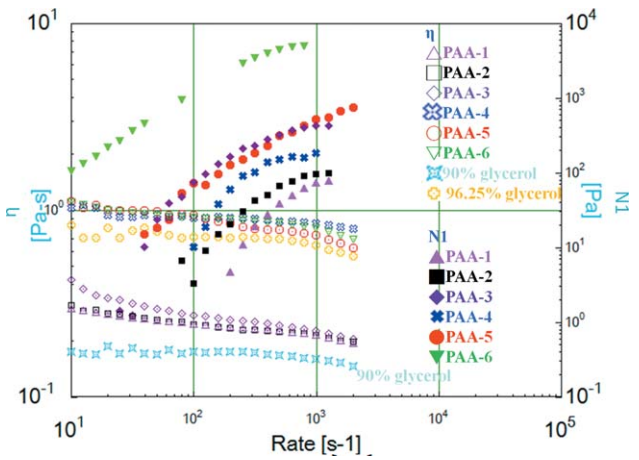

Figure 7. η and N_1 values of the PAA solutions. [Color figure can be viewed in the online issue, which is available at wileyonlinelibrary.com.]

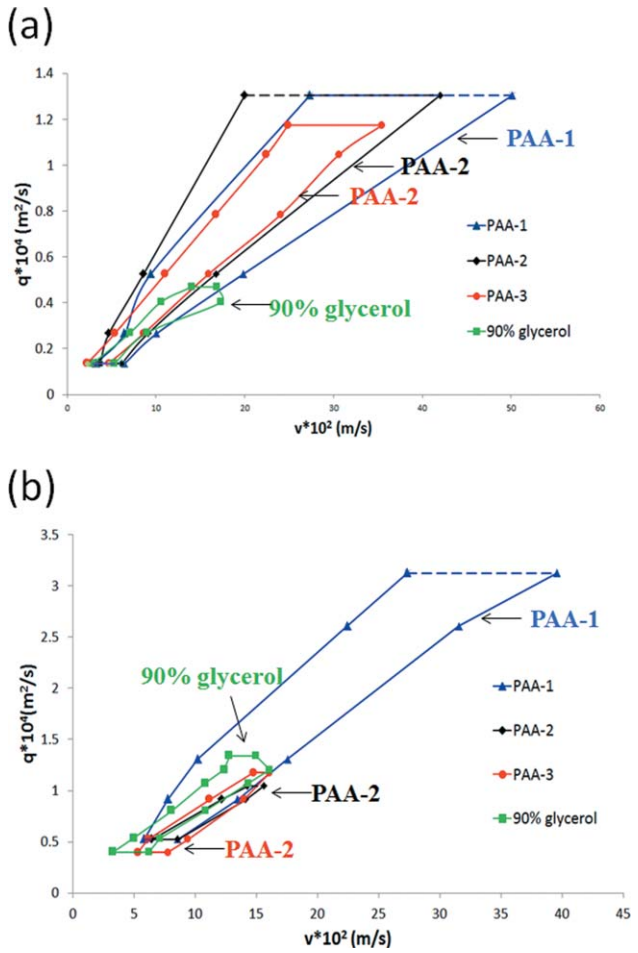

Figure 8. Operating windows of PAA-1 through PAA-3 and 90% glycerol aqueous solutions: H = (a) 400 and (b) 1000 μm. (q is flow rate/unit casting width and v is casting speed) [Color figure can be viewed in the online issue, which is available at wileyonlinelibrary.com.]

The effects of H and the PAA concentration are shown in Figures 8 and 9. For clarity, the results obtained for the six PAA solutions are presented in two figures. As shown in Figure 8(a), the operating windows obtained for the three elastic solutions (PAA-1, PAA-2, and PAA-3) were all larger than those obtained for the Newtonian glycerol solutions with a small H of 400 μm. However, for a larger H of 1000 μm, only the PAA-1 solution showed a substantial increase in the operating window size, as shown in Figure 8(b). A similar behavior was observed for the other three PAA solutions (PAA-4, PAA-5, and PAA-6), as shown in Figure 9. The operating window did not expand continuously with increasing fluid elasticity. It reached a maximum size at a certain optimum elastic level or polymer concentration, beyond which an opposite trend was observed. These results were consistent with those of Ning et al.[34] and Yang et al.[35] on slot die coating. The size of the maximum operating window

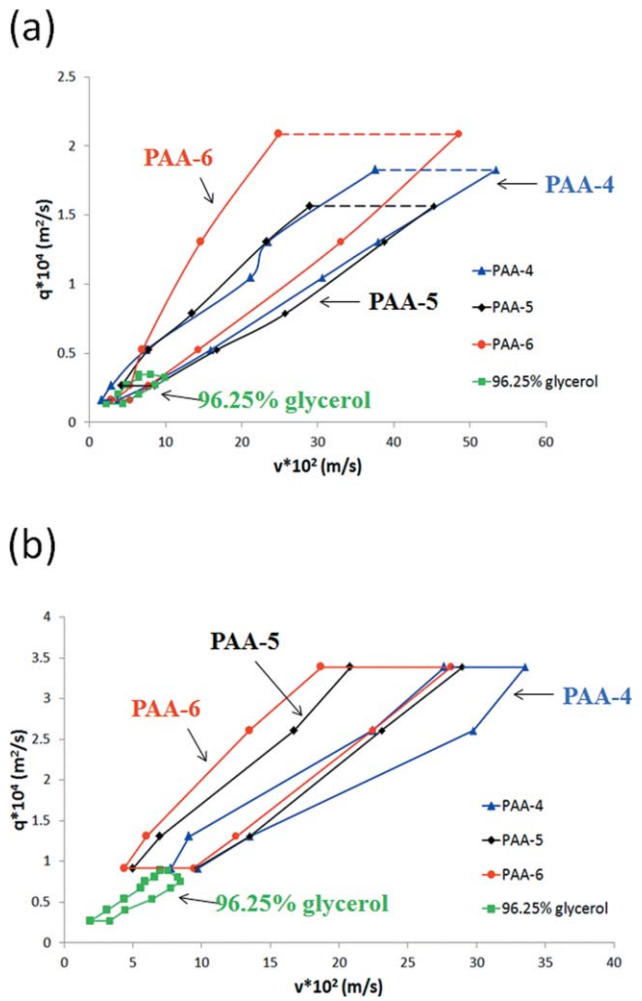

Figure 9. Operating windows of PAA-4 through PAA-6 and 96.25% glycerol aqueous solutions: $H =$ (a) 400 and (b) 1000 μm. (q is flow rate/unit casting width and v is casting speed) [Color figure can be viewed in the online issue, which is available at wileyonlinelibrary.com.]

and the stable coating speed were dependent on the level of fluid elasticity in the flow field or depended indirectly on the polymer concentration and H spacing.

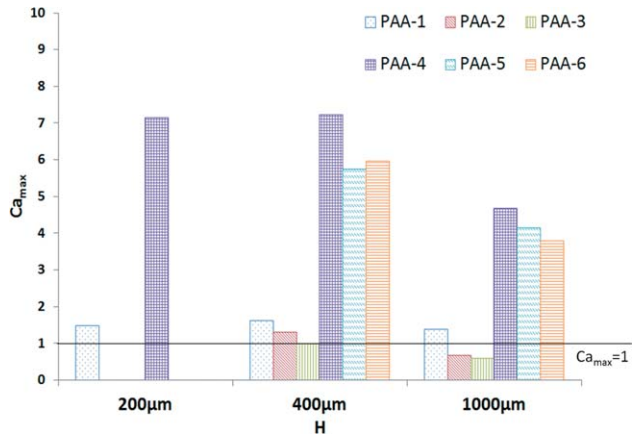

Figure 10. Ca_{max} values of the PAA solutions at V_{max}. [Color figure can be viewed in the online issue, which is available at wileyonlinelibrary.com.]

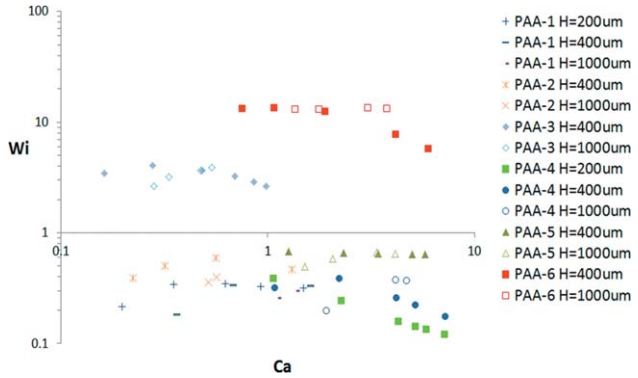

Figure 11. Wi versus Ca for the different PAA solutions. [Color figure can be viewed in the online issue, which is available at wileyonlinelibrary.com.]

Figure 10 shows plots of Ca_{max} versus H for all of the PAA solutions, as shown in Figure 5 for the CMC solutions. The same conclusion could be drawn that the effect of the fluid elasticity on V_{max} was more pronounced when Ca_{max} was greater than unity. It appeared that in the casting viscoelastic solutions, there existed a competitive or synergetic effect between the viscous and elastic forces in stabilizing the flow field between the die and the moving substrate. A small elasticity level in the casting solution was able to assist the viscous drag in stabilizing the flow but not at high elasticity. This phenomenon was discussed in detail in the thesis of Huang.[37] We observed further that the upstream dynamic contact angle was larger with increasing fluid elasticity. Air entrainment occurred when the contact angle approached 180°.

Figure 11 shows plots of Wi against Ca for various PAA solutions. The results were consistent with those of the CMC solutions shown in Figure 6. They also indicated that over a large range of Ca's, Wi was independent of Ca, although a slight downward trend was observed at higher values of Ca. The Wi's for the two concentrated PAA solutions (PAA 3 and PAA 6) were well above unity.

An unusual defect was observed for the concentrated CMC (1500 ppm) and PAA (2000 ppm) solutions. A photo image of this defect is shown in Figure 12. The surface contour was rather rough and distinct from the ribbing defect normally

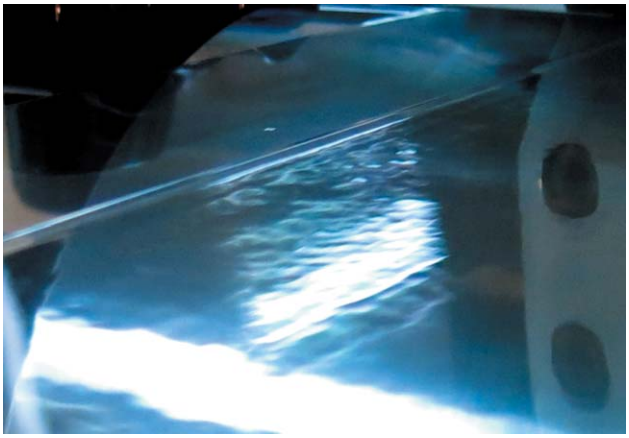

Figure 12. Photo of the rough surface defect. [Color figure can be viewed in the online issue, which is available at wileyonlinelibrary.com.]

observed in purely viscous solutions under the same operating conditions. This new defect was designated as a rough surface. At this stage, it was not clear what caused the appearance of this surface defect. It was reported[38] that the transition from semidilute to concentrated regimes for CMC solutions occurs around 1500 ppm. Without additional fundamental studies, it seems reasonable to assume that the observed rough surface defect could have been due to a combination of chain entanglement, realignment, and breakup of polymer molecules at high shear and in extensional flow fields.

CONCLUSIONS

The operating windows in solution casting with non-Newtonian, viscoelastic CMC and PAA in aqueous glycerol solutions were experimentally investigated. We found that the casting of a shear-thinning fluid with a slight elasticity was able to substantially expand the stable operating windows but not the casting of a fluid with high elasticity. There was a competitive or a synergetic effect between the viscous and elastic forces in controlling the size of the operating window. When Ca was greater than unity, an elastic force exerted by the fluid assisted the viscous force in the expansion of operating window. The strength of the elastic force could be represented in terms of Wi, which was dependent on the MW and molecular structure, and on the polymer concentration. A new rough surface defect was observed for certain concentrated CMC and PAA solutions; this was attributed to the chain entanglement, alignment, or breakup of the polymer molecules.

ACKNOWLEDGMENTS

This research was supported by the National Science Council, Republic of China (contract grant number NSC 98-2221-E-007-010-MY3).

REFERENCES

1. Siemann, U. *Prog. Colloid Polym. Sci.* **2005**, *130*, 1.
2. Shogo, F.; Nagayasu, K.; Masayoshi, S. (to Kaneka Corp.). Jpn. Pat. 2010077311 (**2010**).
3. Asakura, T.; Mizouchi, M.; Kobayashi, H. (to Toray Industries, Inc.). U.S. Pat. 4,470,944 (**1984**).
4. Hamamoto, T.; Inoue, H.; Miwa, Y.; Hirano, T.; Imatani, K.; Matsubara, K.; Kohno, T. (to Ube Industries, Ltd.). U.S. Pat. 5,308,569 (**1994**).
5. Okahashi, M.; Tsukuda, A.; Miwa, T.; Edman, J. R.; Paulson, C. M., II. (to E. I. Du Pont). U.S. Pat. 5,324,475 (**1994**).
6. Takeshi, U.; Noboru, I.; Toshiyuki, N.; Eiji, M.; Keiichi, Y. (to Ube Industries). Jpn. Pat. 2010149494 (**2010**).
7. Yabuta, K.; Akahori, K. (to Kaneka Corp.). U.S. Pat. 6,746,639 (**2004**).
8. Kiyoshi, S.; Shinichi, M. (to Daicel Chemical Industries). Jpn. Pat. 2010163498 (**2010**).
9. Seiji, H.; Masayoshi, S.; Takashi, U.; Nagayasu, K. (to Kaneka Corp.). Jpn. Pat. 2011001439 (**2011**).
10. Hungerford, G. P. (to Mobil Oil Corp.). U.S. Pat. 4,405,550 (**1993**).
11. Kohn, R. S. (to Hoechst Celanese Corp.). U.S. Pat. 4,929,405 (**1990**).
12. Tsujimoto, T. (to Fuji Photo Film Co.). U.S. Pat. 20050110186 (**2005**).
13. Sakamaki, S. (to Fuji Photo Film Co.). WO Pat. 2006101186 (**2006**).
14. Kojyu, I.; Satoshi, S. (to Fujifilm Corp.). U.S. Pat. 20080099954 (**2008**).
15. Miyaji, H. (to Fuji Photo Film Co.). Jpn. Pat. 2006027263 (**2006**).
16. Nakayama, H.; Fukakagawa, N.; Nishiura, Y.; Yasuda, T.; Ito, T.; Mihayashi, K. *J. Photopolym. Sci. Tech.* **2006**, *19*, 169.
17. Akifumi, K.; Hidekazu, Y. (to Fuji Photo Film Co.). Jpn. Pat. 2007090866 (**2007**).
18. Higuchi, J.; Kato, M.; Suzuki, Y. (to Fuji Photo Film Co.). WO Pat. 2006095792 (**2006**).
19. Collins, D. The Story of Kodak; Abrams: New York, **1990**.
20. Steven, J. H.; Lefferts, M. C. (to The Celluloid Co.). U.S. Pat. 573,928 (**1896**).
21. Kinsella, E. (to Celanese Corp.). U.S. Pat. 2,085,532 (**1937**).
22. Machell, J. S.; Greener, J.; Contestable, B. A. *Macromolecules* **1990**, *23*, 186.
23. Greener, J.; Lei, H.; Elman, J.; Chen, J. *J. Soc. Inf. Disp.* **2005**, *13*, 835.
24. Cohen, E. D.; Gutoff, E. B. Modern Coating and Drying Technology; Wiley-Interscience: New York, **1992**; Chapters 1 and 4.
25. Kistler, S. F.; Schweizer, P. M. Liquid Film Coating: Scientific Principles; Their Technological Implications; Chapman & Hall: New York, **1997**; Chapter 11.
26. Chang, Y. R.; Chang, H. M.; Lin, C. F.; Liu, T. J.; Wu, P. Y. *J. Colloid Interface Sci.* **2007**, *308*, 222.
27. Chang, Y. R.; Lin, C. F.; Liu, T. J. *Polym. Eng. Sci.* **2009**, *49*, 1158.
28. Blake, T. D.; Clarke, A.; Ruschak, K. J. *AIChE J.* **1994**, *40*, 229.
29. Blake, T. D.; Dobson, R. A.; Ruschak, K. J. *J. Colloid Interface Sci.* **2004**, *279*, 198.
30. Huang, Y. C.; Wang, T. Z.; Tsai, C. P.; Liu, T. J. *J. Appl. Polym. Sci.* **2013**, *129*, 507.
31. Boger, D. V. J. *Non-Newtonian Fluid Mech. 1997*, *3*, 87.
32. Tam, K. C.; Moussa, T.; Tiu, C. *Rheol. Acta* **1989**, *28*, 112.
33. Davidson, R. L. Handbook of Water-Soluble Gums and Resins; McGraw-Hill: New York, **1980**; Chapter 4.
34. Ning, C. Y.; Tsai, C. C.; Liu, T. J. *Chem. Eng. Sci.* **1996**, *51*, 3289.
35. Yang, C. K.; Wong, D. S. H.; Liu, T. J. *Polym. Eng. Sci.* **2004**, *44*, 1970.
36. Bajaj, M.; Prakash, J. R.; Pasquali, M. *J. Non-Newtonian Fluid Mech.* **2008**, *149*, 104.
37. Huang, Y. C. Ph.D. Thesis, National Tsing Hua University, Taiwan, **2013**.
38. Benchabane, A.; Bekkour, K. *Colloid Polym. Sci.* **2008**, *286*, 1173.